

# UCSF

## UC San Francisco Previously Published Works

### Title

Longitudinal profiling of IDH-mutant astrocytomas reveals acquired RAS-MAPK pathway mutations associated with inferior survival.

### Permalink

<https://escholarship.org/uc/item/9h41g0c3>

### Journal

NOA, 7(1)

### Authors

Rodriguez Almaraz, Eduardo

Guerra, Geno

Al-Adli, Nadeem

et al.

### Publication Date

2025

### DOI

10.1093/noajnl/vdaf024

Peer reviewed

## Longitudinal profiling of IDH-mutant astrocytomas reveals acquired RAS-MAPK pathway mutations associated with inferior survival

Eduardo Rodriguez Almaraz<sup>✉</sup>, Geno A. Guerra<sup>✉</sup>, Nadeem N. Al-Adli, Jacob S. Young, Abraham Dada, Daniel Quintana, Jennie W. Taylor, Nancy Ann Oberheim Bush<sup>✉</sup>, Jennifer L. Clarke<sup>✉</sup>, Nicholas A. Butowski, John de Groot<sup>✉</sup>, Melike Pekmezci, Arie Perry<sup>✉</sup>, Andrew W. Bollen, Aaron W. Scheffler, David V. Glidden, Joanna J. Phillips, Joseph F. Costello, Edward F. Chang, Shawn Hervey-Jumper<sup>✉</sup>, Mitchel S. Berger<sup>✉</sup>, Stephen S. Francis, Susan M. Chang<sup>✉</sup>, and David A. Solomon<sup>✉</sup>

All author affiliations are listed at the end of the article

Corresponding Authors: Susan M. Chang, MD, Division of Neuro-Oncology, University of California, San Francisco, 400 Parnassus Ave, ACC 800, San Francisco, CA 94143, USA ([susan.chang@ucsf.edu](mailto:susan.chang@ucsf.edu)); David A. Solomon, MD, PhD, Department of Pathology, Stanford University, 300 Pasteur Dr, Lane L226, Stanford, CA 94305, USA ([solomond@stanford.edu](mailto:solomond@stanford.edu)).

### Abstract

**Background.** Isocitrate dehydrogenase (IDH)-mutant astrocytomas represent the most frequent primary intraparenchymal brain tumor in young adults, which typically arise as low-grade neoplasms that often progress and transform to higher grade despite current therapeutic approaches. However, the genetic alterations underlying high-grade transformation and disease progression of IDH-mutant astrocytomas remain inadequately defined.

**Methods.** Genomic profiling was performed on 205 IDH-mutant astrocytomas from 172 patients from both initial treatment-naïve and recurrent post-treatment tumor specimens. Molecular findings were integrated with clinical outcomes and pathologic features to define the associations of novel genetic alterations in the RAS-MAPK signaling pathway.

**Results.** Likely oncogenic alterations within the RAS-MAPK mitogenic signaling pathway were identified in 13% of IDH-mutant astrocytomas, which involved the *KRAS*, *NRAS*, *BRAF*, *NF1*, *SPRED1*, and *LZTR1* genes. These included focal amplifications and known activating mutations in oncogenic components (e.g. *KRAS*, *BRAF*), as well as deletions and truncating mutations in negative regulatory components (e.g. *NF1*, *SPRED1*). These RAS-MAPK pathway alterations were enriched in recurrent tumors and occurred nearly always in high-grade tumors, often co-occurring with *CDKN2A* homozygous deletion. Patients whose IDH-mutant astrocytomas harbored these oncogenic RAS-MAPK pathway alterations had inferior survival compared to those with RAS-MAPK wild-type tumors.

**Conclusions.** These findings highlight novel genetic perturbations in the RAS-MAPK pathway as a likely mechanism contributing to the high-grade transformation and treatment resistance of IDH-mutant astrocytomas that may be a potential therapeutic target for affected patients and used for future risk stratification.

### Key Points

- Genetic alterations causing activation of the RAS-MAPK pathway are acquired during progression of IDH-mutant astrocytoma
- Acquisition of RAS-MAPK pathway genetic alterations is associated with inferior survival for patients with IDH-mutant astrocytoma

## Importance of the Study

The genetic events underlying disease progression and high-grade transformation of IDH-mutant astrocytomas have not been fully defined. Here we identified acquisition of genetic alterations activating the RAS-MAPK

pathway in nearly 20% of recurrent IDH-mutant astrocytomas that were associated with inferior survival compared to recurrent tumors lacking RAS-MAPK pathway alteration.

“Astrocytoma, IDH-mutant” is a newly codified tumor type in the 2021 World Health Organization (WHO) Classification of Central Nervous Systems (CNS) Tumors that encompasses a group of diffuse astrocytic gliomas with *IDH1* p.R132 or *IDH2* p.R172 mutation, biallelic *TP53* inactivation, frequent *ATRX* inactivation associated with alternative lengthening of telomeres (ALT), absence of chromosomes 1p and 19q whole arm co-deletion, and a distinct DNA methylation profile.<sup>1</sup> The majority occur in young adults in the third to fifth decades of life, but they can also arise in adolescents and during later adulthood.<sup>2–4</sup> They occur most commonly in the cerebral hemispheres, but can also arise in the cerebellum or brainstem.<sup>5</sup> The majority are sporadic/spontaneous tumors, but they occasionally arise in the setting of specific tumor predisposition syndromes including Li–Fraumeni, Ollier, and Lynch due to constitutional mutations affecting the *TP53*, *IDH1*, and DNA mismatch repair genes (*MSH2*, *MSH6*, *MLH1*, and *PMS2*).<sup>6–8</sup> The majority arise as low-grade tumors (CNS WHO grade 2) which demonstrate slow growth over time. However, IDH-mutant astrocytomas cannot be cured by surgical resection alone given their infiltrative growth that extends beyond what can be visualized by current radiologic methods and what can be safely resected in most patients. While maximal safe resection has a proven survival benefit for these patients, over time IDH-mutant astrocytomas recur and can often transform to higher-grade tumors (CNS WHO grade 3 or 4) with more rapid growth and spread, necessitating repeat surgical resection and/or adjuvant therapies including external beam radiation and chemotherapy, such as with the alkylating agent temozolomide.<sup>9</sup> While they are associated with markedly better survival compared with IDH-wildtype glioblastoma, IDH-mutant astrocytomas are malignant tumors that are not curable with the currently available therapies. However, new therapeutic approaches are on the horizon for affected patients including immunotherapies and the recently U.S. Food and Drug Administration-approved small molecule inhibitors (e.g. vorasidenib) of the mutant isocitrate dehydrogenase (IDH) enzymes encoded by the *IDH1* and *IDH2* genes.<sup>9–11</sup>

IDH-mutant astrocytomas are genetically defined by an activating missense mutation at codon p.R132 in *IDH1* or the analogous codon p.R172 in *IDH2*, which is the earliest initiating oncogenic event in these tumors and fuels gliomagenesis by catalyzing formation of the 2-hydroxyglutarate oncometabolite that underlies the glioma CpG island methylator phenotype.<sup>12,13</sup> Additionally, mutational inactivation of the *TP53* tumor suppressor gene is an early oncogenic event that cooperates with the *IDH1/2* mutation to initiate the formation of an IDH-mutant astrocytoma.<sup>14</sup> As the glioma then expands, inactivating mutation or deletion of the *ATRX* chromatin remodeling

gene is selected for in most tumors that causes ALT to bypass cellular senescence.<sup>15,16</sup> In CNS WHO grade 2 IDH-mutant astrocytomas demonstrating low proliferative activity, absence of anaplasia, and absence of necrosis and microvascular proliferation, the trio of *IDH1/2*, *TP53*, and *ATRX* mutations is typically present without additional accompanying oncogenic alterations.<sup>17</sup> Over time, IDH-mutant astrocytomas acquire additional genetic aberrations that drive high-grade transformation, treatment resistance, and more rapid growth. The additional genetic perturbations that fuel this high-grade transformation are multiple and have been identified through longitudinal profiling studies over the past several years.<sup>18–22</sup> The most frequent additional genetic aberration is homozygous deletion of the *CDKN2A* tumor suppressor gene on chromosome 9p21.3, which encodes the cell cycle regulator p16INK4a. Multiple studies have documented that *CDKN2A* homozygous deletion is enriched in recurrent and high-grade IDH-mutant astrocytomas and correlates with inferior survival compared to IDH-mutant astrocytomas with intact *CDKN2A* alleles.<sup>23–26</sup> As such, the presence of *CDKN2A* homozygous deletion was added as a prognostic grading factor for IDH-mutant astrocytoma in the 2021 WHO Classification, with those tumors harboring this genetic alteration assigned as CNS WHO grade 4 regardless of their histologic features.<sup>1</sup>

Several additional genetic aberrations associated with high-grade transformation and inferior survival of IDH-mutant astrocytomas beyond *CDKN2A* homozygous deletion have been identified. These include aberrations of other cell cycle regulators, such as amplification of *CDK4* (which encodes cyclin-dependent kinase 4), amplification of *CCND2* (cyclin D2), and mutation or deletion of *RB1* (retinoblastoma tumor suppressor).<sup>27–30</sup> The receptor tyrosine kinase genes *PDGFRA* (platelet-derived growth factor receptor alpha) and *MET* (hepatocyte growth factor receptor) are also frequently amplified and rearranged in recurrent and higher-grade IDH-mutant astrocytomas, which are being tested as therapeutic targets in this patient population.<sup>27,31–34</sup> Acquisition of *MYCN* amplification leading to overexpression of the encoded Myc family transcription factor occurs in a small subset of recurrent IDH-mutant astrocytomas that is associated with poor prognosis.<sup>35</sup> Mutations of *PIK3CA* and *PIK3R1* driving hyperactivation of the PI3-kinase-Akt-mTOR signaling pathway were also recently found to occur in a subset of IDH-mutant astrocytomas, particularly recurrent and/or higher-grade tumors associated with inferior survival.<sup>36</sup> Increased burden of chromosomal copy number aberrations across the genome has also been correlated with worse survival among patients with IDH-mutant astrocytomas.<sup>23,37,38</sup> Lastly, recurrent IDH-mutant astrocytomas that develop

somatic hypermutation following chemotherapy with the alkylating agent temozolomide are associated with malignant transformation, poor prognosis, and increased risk of cerebrospinal fluid dissemination.<sup>21,39–41</sup>

To further investigate the molecular events that drive tumor progression and treatment resistance, we performed comprehensive histopathologic assessment and targeted genomic sequencing on 205 IDH-mutant astrocytoma tumor specimens from 172 consecutive patients inclusive of all CNS WHO grades and disease timepoints as part of a sponsored glioma precision medicine program at our institution. We identified the RAS-mitogenic activated protein kinase (MAPK) signaling pathway as a novel target of frequent oncogenic alterations in recurrent IDH-mutant astrocytomas associated with high-grade transformation and inferior survival. We speculate that these RAS-MAPK pathway mutations drive treatment resistance during the progression of IDH-mutant astrocytomas and may serve as a potential therapeutic target for affected patients using specific inhibitors.

## Materials and Methods

### Patient Cohort and Tumor Samples

The study cohort was composed of 205 IDH-mutant astrocytoma tumor specimens from 172 patients who were treated at the University of California, San Francisco (UCSF) Medical Center between 2015 and 2023. All patients had tumors pathologically confirmed as “Astrocytoma, IDH-mutant” according to the 2021 WHO Classification of Central Nervous System Tumors based on the combination of histopathologic features and targeted next-generation DNA sequencing (NGS) including assessment of gene mutations, fusions and other structural variants, and chromosomal copy number profiles. Specifically, all tumors were diffuse astrocytic gliomas located supratentorially in the cerebral hemispheres and were confirmed to be IDH-mutant with either *IDH1* p.R132 or *IDH2* p.R172 missense mutations detected by NGS. All tumors lacked whole arm co-deletion of chromosomes 1p and 19q and were histone H3-wildtype (e.g. lacked p.K27 or p.G34 mutation in *H3-3A*, *H3-3B*, *H3C2*, and *H3C3*). In total, 205 tumor specimens from the 172 included patients were examined by histopathology and genomic profiling. This included 95 initial treatment-naive tumor specimens from an initial diagnostic surgical resection, and 110 recurrent tumor specimens from a subsequent surgical resection following either observation or adjuvant therapy. For 24 patients, there were multiple longitudinal tumor specimens that were genomically profiled. While a subset of patients was treated with an IDH mutant small molecule inhibitor (either vorasidenib, ivosidenib, or enasidenib) at the time of disease progression ( $n = 13$ ), no patients in this cohort were treated with an IDH mutant small molecule inhibitor in the adjuvant setting following the initial diagnostic surgery, and all genomic profiling was performed prior to therapy with IDH mutant small molecule inhibitors. This study was approved by the institutional review board of the University of California, San Francisco. As part of routine clinical practice at UCSF, all patients included in the study

cohort signed an informed consent waiver to contribute de-identified data to scientific research projects.

### Histology and Immunohistochemistry

All tumors were pathologically confirmed as IDH-mutant astrocytoma based on a combination of immunoreactivity for IDH1 R132H mutant protein, NGS results showing the presence of *IDH1* p.R132 or *IDH2* p.R172 variants, and chromosomal copy number status showing absence of whole arm co-deletion of chromosomes 1p and 19q. Detailed pathologic examination was performed retrospectively to investigate histologic and immunohistochemical features of the IDH-mutant astrocytoma cohort, including both histologic grading based on the 2016 WHO Classification and integrated grading based on the 2021 WHO Classification. Immunohistochemistry was performed on whole formalin-fixed, paraffin-embedded tissue sections using the following antibodies: IDH1 R132H mutant protein (Dianova, clone H09, 1:500 dilution, ER2 antigen retrieval), p53 (Biocare, clone DO-7, 1:100 dilution, ER2 antigen retrieval), ATRX (Sigma, polyclonal, 1:100 dilution), histone H3 K27M mutant protein (RevMab Biosciences, clone RM192, 1:600 dilution), histone H3 lysine 27 trimethylation (Cell Signaling, clone C36B11, 1:50 dilution, ER2 antigen retrieval), histone H3.3 G34R mutant protein (RevMab Biosciences, clone RM240, 1:100 dilution), Ki-67 (Dako, clone Mib1, 1:50 dilution, ER2 antigen retrieval), and phosphorylated p44/42 ERK1/2 Thr202/Tyr204 (Cell Signaling, clone D13.14.4E, 1:10 000 dilution). Tissue sections used for phospho-ERK1/2 immunohistochemistry included both a subset of the tumors with oncogenic RAS-MAPK alterations ( $n = 12$ ), adjacent uninvolved cortex from tumors with oncogenic RAS-MAPK alterations ( $n = 10$ ), and IDH-mutant astrocytomas lacking identifiable RAS-MAPK pathway alterations (RAS-MAPK wildtype,  $n = 6$ ). Immunostaining was performed in Leica Bond-Max or Ventana BenchMark Ultra automated stainers. Diaminobenzidine was used as the detection chromogen, followed by hematoxylin counterstain.

### Targeted Next-Generation DNA Sequencing

Genomic DNA was extracted from formalin-fixed, paraffin-embedded tumor tissue of 205 longitudinal IDH-mutant astrocytoma tumor specimens from the 172 patients using the QIAamp DNA FFPE Tissue Kit (Qiagen). Tumor tissue was selectively scraped from unstained slides or punched from formalin-fixed, paraffin-embedded blocks using biopsy punches (Integra Miltex Instruments) to enrich for high tumor content. For a subset of patients,  $n = 49$  as indicated, a constitutional DNA sample was extracted from a buccal swab or peripheral blood specimen using the QIAamp DNA Blood Midi Kit (Qiagen) and simultaneously sequenced to enable accurate discrimination of germline/constitutional versus somatic origin of variants. Capture-based next-generation DNA sequencing was performed using the UCSF500 NGS panel as previously described that targets all coding exons of 529 cancer-related genes, select introns, and upstream regulatory regions of 73 genes to enable the detection of structural variants including gene fusions, and DNA segments at regular

intervals along each chromosome to enable genome-wide copy number and zygosity analysis, with a total sequencing footprint of 2.8 Mb.<sup>42–46</sup> Multiplex library preparation was performed using the KAPA Hyper Prep Kit (Roche) according to the manufacturer's specifications using 200 ng of sample DNA. Hybrid capture of pooled libraries was performed using a custom oligonucleotide library (Integrated DNA Technologies). Captured libraries were sequenced as paired-end reads on an Illumina NovaSeq 6000 instrument. Sequence reads were mapped to the reference human genome build GRCh37 (hg19) using the Burrows-Wheeler aligner. Recalibration and deduplication of reads were performed using the Genome Analysis Toolkit. Coverage and sequencing statistics were determined using Picard CalculateHsMetrics and Picard CollectInsertSizeMetrics. Single nucleotide variant and insertion/deletion mutation calling was performed with Mutect2, FreeBayes, Unified Genotyper, and Pindel. Structural rearrangement calling was performed with Delly. Single nucleotide variants, insertions/deletions, and structural variants were visualized and verified using Integrative Genome Viewer. Genome-wide copy number and zygosity analysis was performed by CNVkit<sup>47</sup> and visualized using Nexus Copy Number (Biodiscovery). Microsatellite instability determination was performed with MSIsensor2 analysis of mononucleotide and dinucleotide repeats.<sup>48</sup> Astrocytomas were deemed positive for microsatellite instability when  $\geq 10\%$  of the 86 microsatellites assessed by the UCSF500 NGS panel were unstable. Somatic tumor mutation burden (TMB) was determined by calculating the number of somatic mutations in the coding regions of genes in the UCSF500 NGS panel, counting both single nucleotide variants and short indels, divided by the total coding footprint of the assay (1.5 Mb). For patients with paired tumor-normal sequencing performed, TMB was calculated using only the confirmed somatic mutations. For patients with tumor-only sequencing performed, TMB was calculated by removing known germline variants present at  $\geq 0.001\%$  frequency in human population datasets (ExAC, gnomAD, and NHLBI-ESP6515). Hypermutation was defined as those tumors with TMB values of  $\geq 10$  somatic mutations per Mb based on this assay. Temozolomide-induced hypermutation corresponding to single base substitution mutational signature 11 from the COSMIC Human Cancer Mutational Signatures Database version 3.4 was defined as those recurrent astrocytomas demonstrating somatic hypermutation acquired following chemotherapy with temozolomide characterized by a preponderance of C>T/G>A transitions.<sup>21,41,49,50</sup> Each of the confirmed somatic variants from paired tumor-normal sequencing or filtered variants from tumor-only sequencing analysis was reviewed for predicted oncogenicity/pathogenicity using known cancer genomics data in the COSMIC (<http://cancer.sanger.ac.uk/cosmic>) and cBioPortal (<http://www.cbioportal.org/>) databases, location within encoded protein, and predicted functional effect based on mutation type (e.g. missense, nonsense, frameshift, splice site).

### RAS-MAPK Pathway Genetic Analysis

Somatic genetic alterations either known or predicted to cause activation of the RAS-MAPK signaling pathway were identified in the targeted DNA sequencing data from

the IDH-mutant astrocytoma cohort. RAS-MAPK pathway genes evaluated for genetic alterations included *KRAS*, *NRAS*, *BRAF*, *NF1*, *SPRED1*, *PTPN11*, and *LZTR1*. This analysis included assessment for focal amplification events, activating missense variants, or structural variants/fusions targeting the oncogenic components *KRAS*, *NRAS*, *BRAF*, and *PTPN11*, as well as assessment for focal deletion events, truncating indel mutations or structural variants, or deleterious missense variants targeting the negative regulatory components *NF1*, *SPRED1*, and *LZTR1*.<sup>51–53</sup> For survival analysis, patients were classified as RAS-MAPK wildtype or RAS-MAPK altered based on the presence or absence of known or likely oncogenic/pathogenic variants targeting these key genes: *KRAS*, *NRAS*, *BRAF*, *NF1*, *SPRED1*, *PTPN11*, and/or *LZTR1*.

### Statistical Analysis

All analyses were conducted using the statistical software R version 4.2.3. Patient demographics and tumor characteristics were summarized using descriptive statistics. Student's *t*-test, Fisher's exact test, and Chi-squared tests were employed to compare continuous and categorical variables between patient groups stratified by RAS-MAPK alterations. Overall survival from initial surgery was defined as the time from the initial diagnostic surgical procedure to death. Survival from surgically treated recurrence was defined as the time from repeat resection for pathologically confirmed viable recurrent IDH-mutant astrocytoma until death. Kaplan–Meier plots were used to estimate survival times stratified by clinical and molecular variables, with censoring performed for patients alive at the last clinical follow-up. Median estimated survival with 95% confidence intervals (CI) and exact *P*-values were calculated by log-rank test. Univariate and multivariate Cox proportional hazards regression models were used to evaluate the associations between clinical and molecular factors with survival outcomes. Multivariate models were constructed using variables determined a priori.

## Results

### IDH-Mutant Astrocytoma Patient Cohort

The study cohort consisted of 172 patients (61% male, 39% female) with pathologically confirmed IDH-mutant astrocytoma who underwent surgical resection of one or more longitudinal tumor specimens that were genomically profiled (Table 1, Supplementary Table S1). In total, 205 tumor specimens were included, consisting of 95 treatment-naïve tumors from an initial diagnostic surgical resection and 110 recurrent tumors from a subsequent surgical resection following either observation or adjuvant therapy. The median age at initial diagnosis for the 172 patients was 33.2 years (range 10.1–67.0 years). The tumors were uniformly supratentorial located in the cerebral hemispheres. Dependent on clinical factors including residual disease after resection and tumor grade, a subset of patients was observed by follow-up magnetic resonance imaging (MRI) without adjuvant therapy, while

**Table 1.** Study Cohort of Patients With Sporadic IDH-Mutant Astrocytomas Stratified by Presence/Absence of Likely Oncogenic Alterations Within RAS-MAPK Pathway Genes (*KRAS*, *NRAS*, *BRAF*, *NF1*, *SPRED1*, *PTPN11*, and *LZTR1*)

<i>n</i> (%)	Initial Treatment-Naïve Sporadic IDH-Mutant Astrocytoma				Recurrent Sporadic IDH-Mutant Astrocytoma			
	Total 90	RAS-MAPK Pathway Mutant 8 (9)	RAS-MAPK Pathway Wildtype 82 (91)	<i>P</i> -Value	Total 109	RAS-MAPK Pathway Mutant 18 (17)	RAS-MAPK Pathway Wildtype 91 (83)	<i>P</i> -Value
Sex, <i>n</i> (%)				.48				.83
Female	40 (44)	5 (63)	35 (43)		35 (32)	6 (33)	29 (32)	
Male	50 (56)	3 (37)	47 (57)		74 (68)	12 (67)	62 (68)	
Age at initial diagnosis, mean (SD)	35.7 (12.5)	39.7 (7.1)	35.3 (12.8)	.15	33.8 (8.5)	32.9 (10.0)	34 (8.2)	.65
Tumor location, <i>n</i> (%)				1				1
Cerebral hemispheres	90 (100)	8 (100)	82 (100)		109 (100)	18 (100)	91 (100)	
Brainstem/spinal cord	0 (0)	0 (0)	0 (0)		0 (0)	0 (0)	0 (0)	
Cerebellum	0 (0)	0 (0)	0 (0)		0 (0)	0 (0)	0 (0)	
Lobe location, <i>n</i> (%)				.66				.61
Frontal	54 (60)	3 (38)	51 (62)		51 (47)	6 (33)	45 (50)	
Temporal	12 (13)	2 (26)	10 (12)		26 (24)	5 (28)	21 (23)	
Parietal	10 (11)	1 (12)	9 (11)		18 (17)	2 (11)	14 (15)	
Occipital	1 (1)	0 (0)	1 (1)		2 (2)	0 (0)	1 (1)	
Frontotemporal	9 (10)	1 (12)	8 (10)		9 (8)	2 (11)	6 (7)	
Frontoparietal	3 (3)	1 (12)	2 (2)		1 (1)	0 (0)	1 (1)	
Parietooccipital	1 (1)	0 (0)	1 (1)		0 (0)	0 (0)	0 (0)	
Temporoparietal	0 (0)	0 (0)	0 (0)		1 (1)	3 (17)	2 (2)	
Temporooccipital	0 (0)	0 (0)	0 (0)		1 (1)	0 (0)	1 (1)	
Histologic grade per 2016 WHO classification, <i>n</i> (%)				.39				.33
Grade II	30 (33)	1 (13)	29 (35)		17 (16)	2 (11)	15 (17)	
Grade III	22 (24)	3 (37)	19 (23)		22 (20)	2 (11)	20 (22)	
Grade IV	38 (42)	4 (50)	34 (42)		70 (64)	14 (78)	56 (61)	
2021 CNS WHO classification grade, <i>n</i> (%)				.42				.31
Grade 2	30 (33)	1 (12)	29 (35)		13 (12)	1 (5)	12 (13)	
Grade 3	19 (21)	2 (25)	17 (21)		20 (18)	2 (11)	18 (20)	
Grade 4	41 (46)	5 (63)	36 (44)		76 (70)	15 (84)	61 (67)	
Extent of resection at initial surgery, <i>n</i> (%)				.69				.69
Biopsy only	6 (7)	0 (0)	6 (7)		7 (6)	2 (11)	5 (5)	
Subtotal	57 (63)	5 (63)	52 (63)		21 (19)	3 (17)	18 (20)	
Gross total	27 (30)	3 (37)	24 (30)		81 (74)	13 (72)	68 (75)	
Adjuvant radiation after initial surgery, <i>n</i> (%)				.41				.61
Yes	50 (64)	6 (86)	44 (62)		63 (60)	10 (56)	53 (61)	
No	28 (36)	1 (14)	27 (38)		42 (40)	8 (44)	34 (39)	
Unknown	12	1	11		4	0	4	
Adjuvant temozolomide after initial surgery, <i>n</i> (%)				.25				.61
Yes	49 (63)	6 (86)	43 (60)		63 (60)	10 (56)	53 (61)	
No	29 (37)	1 (14)	28 (40)		42 (40)	8 (44)	34 (39)	
Unknown	12	1	11		4	0	4	

Table 1. Continued

n (%)	Initial Treatment-Naïve Sporadic IDH-Mutant Astrocytoma				Recurrent Sporadic IDH-Mutant Astrocytoma			
	Total 90	RAS-MAPK Pathway Mutant 8 (9)	RAS-MAPK Pathway Wildtype 82 (91)	P-Value	Total 109	RAS-MAPK Pathway Mutant 18 (17)	RAS-MAPK Pathway Wildtype 91 (83)	P-Value
Overall survival from initial surgery (years), median (95% CI)					.59			
	8.0 (7.5–NA)	8.0 (NA–NA)	12.1 (7.5–NA)		N/A	N/A	N/A	
Overall survival from surgically treated recurrence (years), median (95% CI)								
	N/A	N/A	N/A		3.2 (2.8–4.9)	1.2 (0.8–NA)	3.5 (2.6–5.1)	.01

Significant *P*-values < .05 are in bold.

others received adjuvant external beam radiation and/or adjuvant cycles of chemotherapy with temozolomide. While a subset of patients was treated with an IDH mutant small molecule inhibitor (either vorasidenib, ivosidenib, or enasidenib) at the time of disease progression ( $n = 13$ ), no patients in this cohort were treated with an IDH mutant small molecule inhibitor in the adjuvant setting following the initial diagnostic surgery, and all genomic profiling was performed prior to therapy with IDH mutant small molecule inhibitors. The median overall survival from initial diagnostic surgery was 11.8 years (95% CI: 9.9–15.5 years), and the median follow-up time was 5.5 years. Individual genetic alterations known to be associated with inferior survival in IDH-mutant astrocytomas including *CDKN2A* homozygous deletion and *PDGFRA* amplification were observed to correlate with worse survival in this patient cohort (data not shown). Among 81 genomically profiled recurrent IDH-mutant astrocytomas following preceding treatment with temozolomide, 14 tumors (17%) demonstrated somatic hypermutation composed almost entirely of C>T:G>A transitions corresponding with single base substitution signature 11 in the COSMIC Human Cancer Mutational Signatures Database version 3.4 and harbored a high frequency (79%) of mismatch repair genes mutations involving *MSH2*, *MSH6*, *MLH1*, or *PMS2*.

### Clinical Subtypes of IDH-Mutant Astrocytomas

Among the 172 patients, 49 patients underwent simultaneous sequencing of a matched constitutional DNA sample extracted from peripheral blood or buccal swab, as dictated by either patient request or clinical indication based on personal or family history of malignancy. Five patients (3%) had confirmed constitutional variants (2 in *TP53*, 1 in *IDH1*, and 2 in *MSH2*), diagnostic of IDH-mutant astrocytoma arising in the setting of Li-Fraumeni, Ollier, and Lynch syndromes, respectively. See [Supplementary Results](#) for a detailed description of these 5 patients with syndromic IDH-mutant astrocytomas. The other 44 patients

lacked deleterious constitutional variants in genes known to be associated with glioma predisposition including *TP53*, *CDKN2A*, *NF1*, *IDH1*, and the mismatch repair genes (*MSH2*, *MSH6*, *MLH1*, and *PMS2*), with all identified oncogenic mutations in the tumor specimens confirmed to be somatic (i.e. tumor acquired), and were thus designated as having sporadic non-syndromic IDH-mutant astrocytomas. The other 123 patients had likely sporadic tumors as well, but did not have constitutional testing performed for definitive confirmation. A Kaplan-Meier plot of survival for the patients with IDH-mutant astrocytomas stratified by clinical subtype as sporadic/non-syndromic versus arising in these different syndromes is shown in [Figure 1B](#) to provide visualization of outcome lengths (no statistical comparison performed given small cohort sizes).

### Novel RAS-MAPK Pathway Alterations in IDH-Mutant Astrocytomas Associated With High-Grade Features

Through genomic profiling of 205 IDH-mutant astrocytomas from 172 patients, we identified genetic alterations of the RAS-MAPK signaling pathway in 27 tumors (13%) that has not been previously identified as a target of frequent genetic alterations in this tumor type ([Table 1](#), [Figures 1–4](#), [Supplementary Figure S1](#), [Supplementary Tables S2–S4](#)). These were all genetic alterations either known or likely to be oncogenic and activating of RAS-MAPK signaling and involved multiple genes in the pathway including *KRAS*, *NRAS*, *BRAF*, *NF1*, *SPRED1*, and *LZTR1*, often in a mutually exclusive manner with each tumor usually harboring an event in one of the genes. No IDH-mutant astrocytomas in this cohort had activating mutations within *PTPN11*, a RAS-MAPK pathway gene that is a frequent target of activating mutations in other glioma tumor types including IDH-wildtype glioblastoma and rosette-forming glioneuronal tumor.<sup>43,54</sup> The identified variants within the RAS-MAPK pathway in this cohort of IDH-mutant astrocytomas were diverse and included

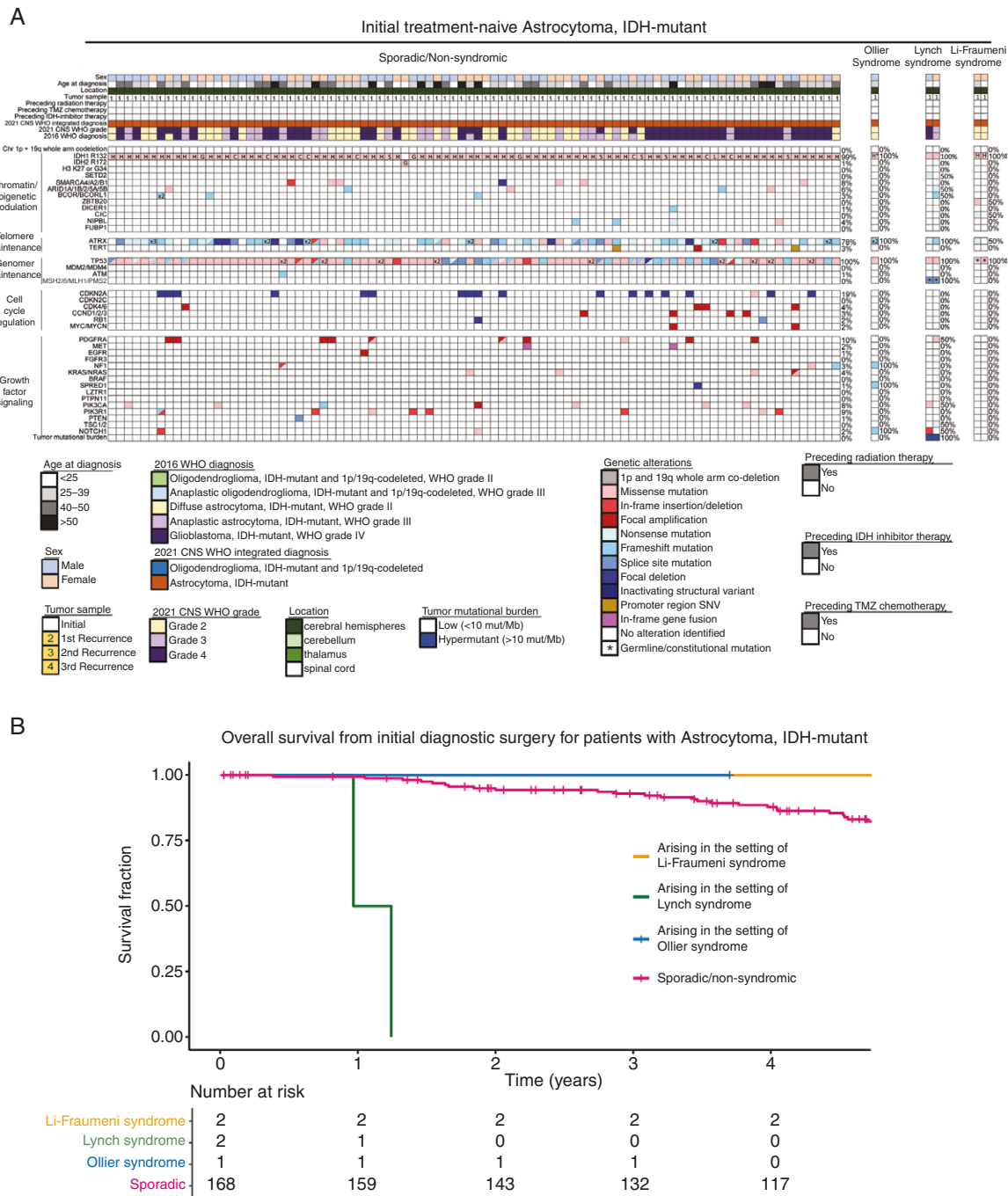


**Figure 1.** IDH-mutant astrocytomas can be classified into multiple clinical subtypes as either sporadic/non-syndromic or arising in the setting of Li-Fraumeni syndrome, Lynch syndrome, or Ollier syndrome. (A) Oncoprint summary plot of the 95 patients with initial treatment-naive IDH-mutant astrocytoma stratified by subtypes. (B) Kaplan-Meier plot of overall survival from initial diagnostic surgery for the total cohort of 172 patients with astrocytoma, IDH-mutant stratified by subtypes.

known oncogenic missense mutations in *KRAS* and *NRAS* ( $n = 8$ , including p.G12D, p.G12V, p.G12A, p.G13D, p.G13S, p.D33E, p.K117N, and p.A146T), focal high-level amplification of *KRAS* ( $n = 3$ ), known oncogenic missense mutations in *BRAF* ( $n = 2$ , p.G464E, p.D594G), in-frame *BRAF* gene fusion ( $n = 1$ ), truncating (nonsense, frameshift, splice site) mutations or known deleterious missense

mutations in *NF1* and *LZTR1* ( $n = 17$  and  $4$ , respectively), and focal homozygous/biallelic deletion or truncating frameshift mutation of *SPRED1* ( $n = 2$ ). The *BRAF* gene fusion linked the N-terminal exons 1–17 of *PTPRZ1* with the C-terminal exons 11–18 of *BRAF* that encode the serine/threonine kinase domain. *PTPRZ1* is a rare fusion partner of *BRAF* that has been previously encountered in pilocytic

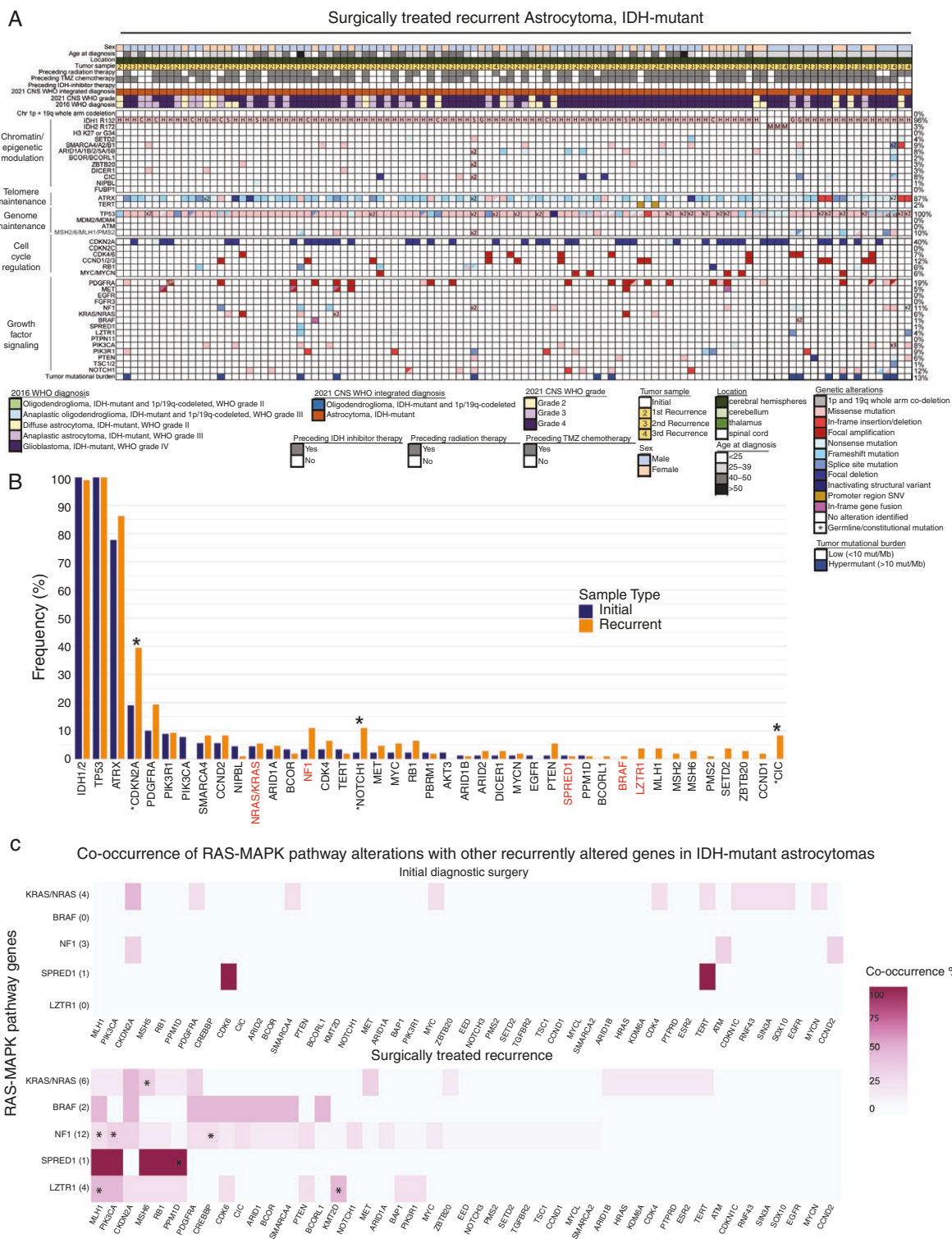


**Figure 2.** Recurrent IDH-mutant astrocytomas are enriched with *CDKN2A* homozygous deletion and diverse RAS-MAPK pathway oncogenic alterations. (A) Oncoprint summary plot for the 110 surgically treated recurrent IDH-mutant astrocytomas which were all sporadic/non-syndromic. Recurrent IDH-mutant astrocytomas with hypermutation defined as tumor mutation burden values of  $\geq 10$  somatic mutations per Mb following temozolomide treatment with single base substitution mutational signature 11 (COSMIC Human Cancer Mutational Signatures Database version 3.4) composed of a predominance of C>T/G>A transitions are denoted. (B) Bar plot of oncogenic alteration frequency for the most commonly altered genes in sporadic IDH-mutant astrocytomas segregated by 90 initial treatment-naive tumors versus 110 surgically treated recurrent tumors. Asterisks denote those individual genes with significantly ( $P < .05$ ) increased alteration frequency at recurrence. (C) Co-occurrence heatmap of RAS-MAPK pathway alterations with other recurrently altered genes in sporadic IDH-mutant astrocytomas segregated by initial treatment-naive tumors vs. surgically treated recurrent tumors. Asterisks denote significantly ( $P < .01$ ) co-occurring genetic alterations by Fisher’s exact test.

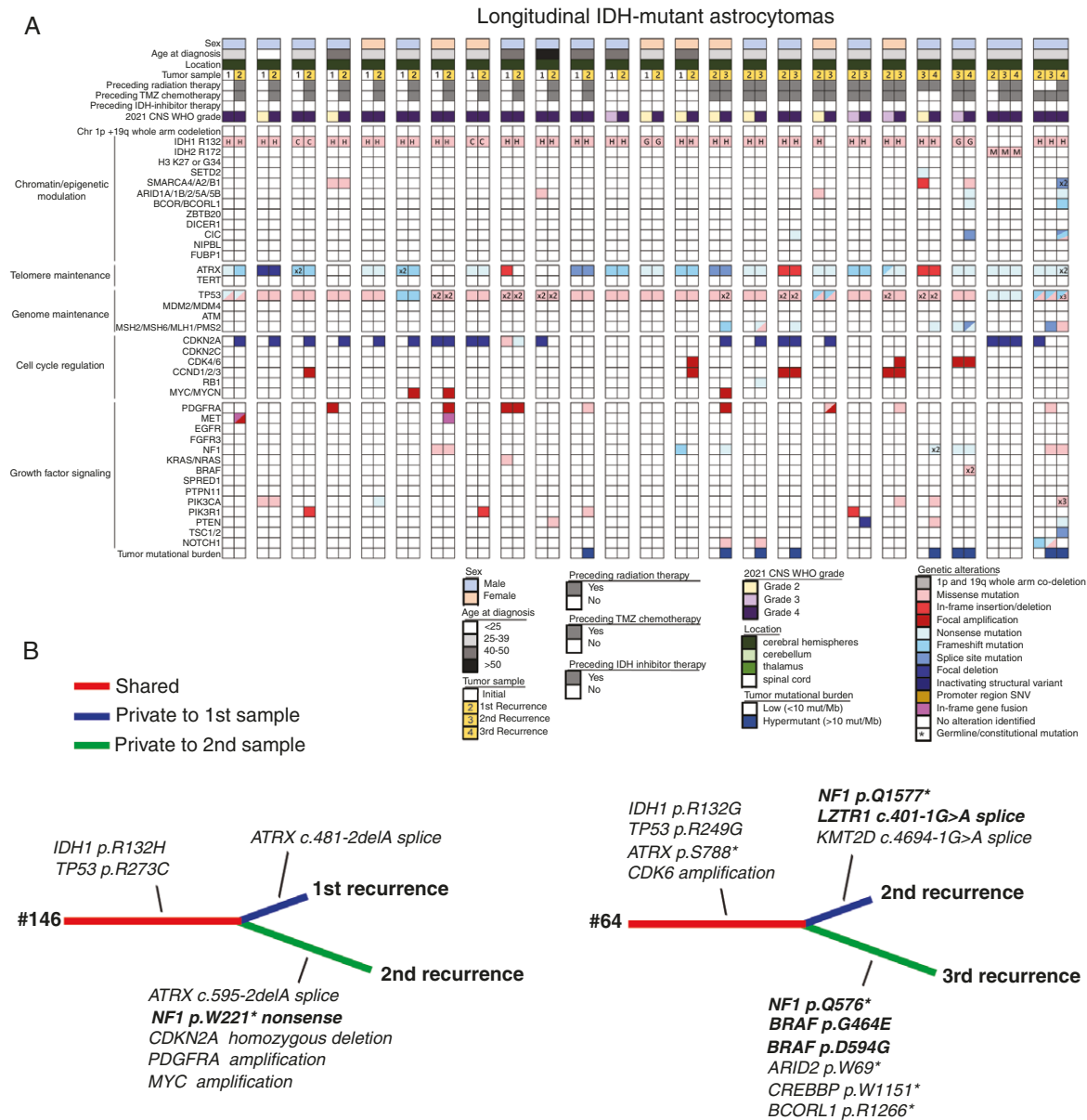


**Figure 3.** Longitudinal genomic profiling of IDH-mutant astrocytomas reveals acquisition of *CDKN2A* homozygous deletion and diverse RAS-MAPK pathway oncogenic alterations in recurrent high-grade tumors. (A) Oncoprint summary plot of the 50 sporadic IDH-mutant astrocytomas from 24 patients that were longitudinally profiled. (B) Genetic evolution dendrograms for patients with longitudinally profiled IDH-mutant astrocytoma demonstrating new acquisition of RAS-MAPK alterations at recurrence.

astrocytoma.<sup>55</sup> All variants in RAS-MAPK genes were either confirmed as somatic by paired tumor-normal sequencing or by longitudinal profiling of multiple temporally-spaced tumor specimens with variants private to individual tumor specimens, or they were present in tumor specimens analyzed as tumor-only at variant allele frequencies consistent with probable somatic origin.

We performed immunohistochemistry for phosphorylated Thr202 and Tyr204 isoforms of ERK1/2 on IDH-mutant astrocytomas with and without RAS-MAPK pathway mutations to further investigate the status of the signaling pathway downstream of these genetic events (Figure 4).

We observed minimal to absent phospho-ERK1/2 labeling in normal cortex and IDH-mutant astrocytomas with no identifiable RAS-MAPK pathway genetic alterations (RAS-MAPK wildtype). In contrast, we observed robust phospho-ERK1/2 positivity in IDH-mutant astrocytomas containing the diverse oncogenic alterations within the RAS-MAPK component genes. This finding provides protein-level evidence that these RAS-MAPK genetic alterations were causing activation of this mitogenic signaling pathway in a subset of IDH-mutant astrocytomas.

Among the 26 sporadic non-syndromic IDH-mutant astrocytomas with likely oncogenic variants affecting the

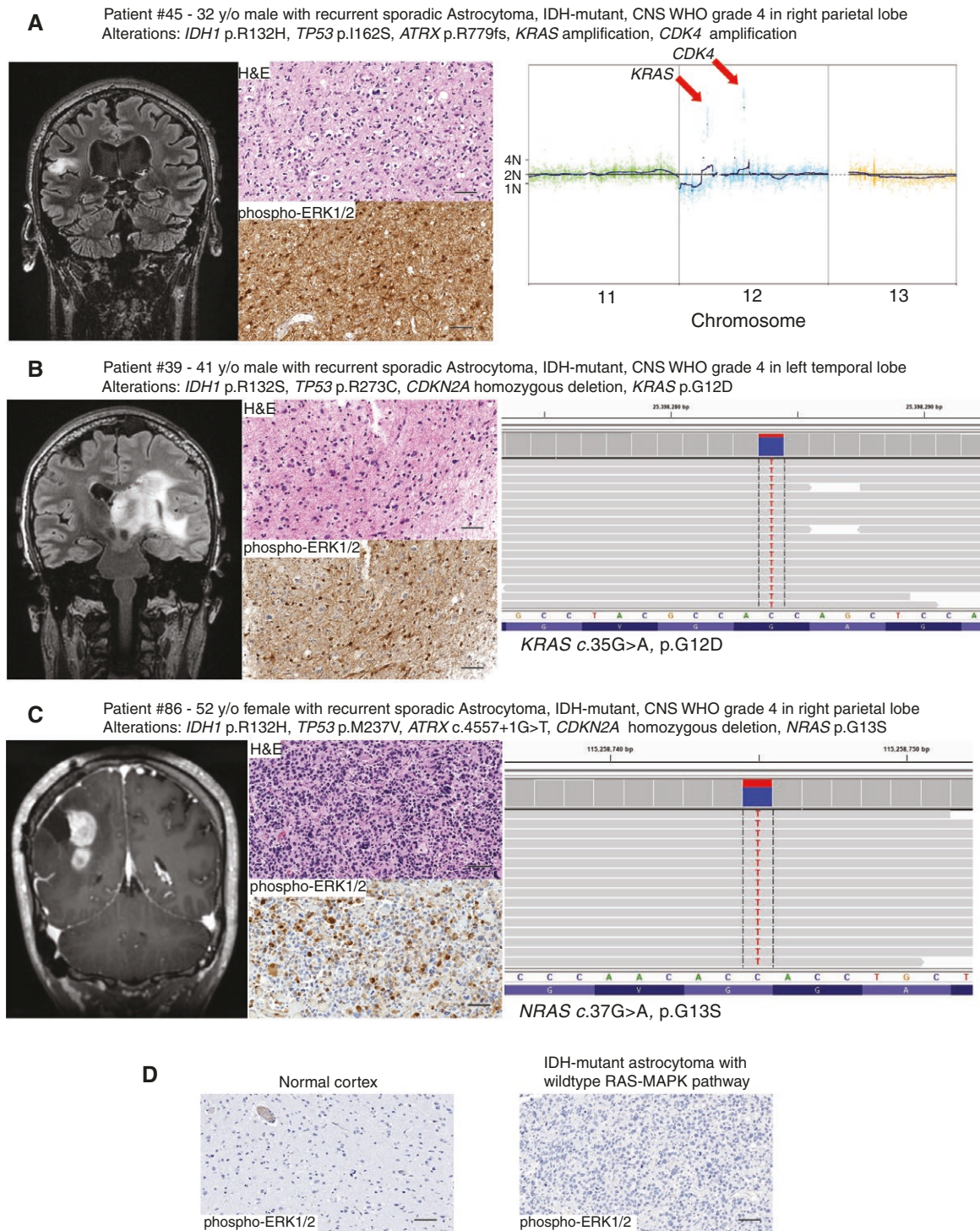


**Figure 4.** Diverse RAS-MAPK pathway oncogenic alterations in recurrent high-grade sporadic IDH-mutant astrocytomas. Shown are 3 representative patients, including a coronal T1 post-contrast MR image, hematoxylin and eosin-stained histology image, phospho-ERK1/2 Thr202/Tyr204 immunostaining, and a snapshot of the oncogenic RAS-MAPK alterations. (A) Focal high-level amplification of the *KRAS* oncogene on chromosome 12p12.1. (B) *KRAS* p.G12D known activating hotspot missense mutation. (C) *NRAS* p.G13S known activating hotspot missense mutation. (D) Phospho-ERK1/2 Thr202/Tyr204 immunostaining of normal cortex and an IDH-mutant astrocytoma with wildtype RAS-MAPK pathway. Scale bar, 100 microns.

RAS-MAPK signaling pathway, 8 were in the cohort of 90 initial treatment-naive tumors (9% frequency, Figure 1A) and 18 were in the cohort of 109 recurrent tumors (17% frequency, Figure 2A and B). The oncogenic RAS-MAPK pathway mutations frequently co-occurred with *CDKN2A* homozygous deletion and *PIK3CA* mutation (Figure 2A and C). Longitudinal genomic profiling of multiple tumor samples from individual patients revealed that these RAS-MAPK pathway mutations occurred during tumor progression after the initiating truncal *IDH1*, *TP53*, and *ATRX* mutational events (Figure 3). For example in patient #146, a private *NF1* truncating nonsense mutation was newly acquired in the second recurrence tumor specimen that was not present in the prior first recurrence (Figure 3B). In patient #64, both the second and third recurrence tumor specimens harbored *NF1* truncating nonsense mutations that were 2 different early-stop mutations affecting divergent codons in the *NF1* gene, thereby indicating these mutations were private and newly acquired in each of the tumor specimens. These *NF1* mutations were accompanied by additional private *LZTR1* splice site mutation in the second recurrence and 2 private *BRAF* missense mutations in the third recurrence (Figure 3B).

There were no differences in sex, age at diagnosis, or tumor location among the patients whose tumors did or did not have RAS-MAPK pathway alterations (Table 1). Nearly all IDH-mutant astrocytomas with RAS-MAPK pathway alterations had high-grade histologic features (Table 1). Among the 8 initial treatment-naive tumors, 4 had either necrosis or microvascular proliferation (WHO grade IV per 2016 WHO Classification criteria) and 3 had anaplasia and increased mitotic activity only (WHO grade III per 2016 WHO Classification criteria). Only 1 tumor lacked appreciable high-grade histologic features. Among the 18 recurrent tumors, 14 had either necrosis or microvascular proliferation (WHO grade IV per 2016 WHO Classification criteria) and 4 had anaplasia and increased mitotic activity only (WHO grade III per 2016 WHO Classification criteria), with only 2 tumors lacking appreciable high-grade histologic features. When accounting for the molecularly integrated 2021 WHO Classification criteria that includes *CDKN2A* homozygous deletion into the grading scheme, only 1 initial treatment-naive tumor remained at CNS WHO grade 2 and only 1 recurrent tumor remained at CNS WHO grade 2, with the other 24 tumors all assigned as high-grade (20 as CNS WHO grade 4 and 4 as CNS WHO grade 3). Thus, there was a substantial enrichment of RAS-MAPK oncogenic alterations in high-grade IDH-mutant astrocytomas in this cohort ( $P < .05$  by Chi-squared test), with the majority being CNS WHO grade 4 based on co-occurring *CDKN2A* homozygous deletion and/or necrosis and microvascular proliferation histologically.

### Recurrent IDH-Mutant Astrocytomas With Oncogenic RAS-MAPK Pathway Alterations are Associated With Inferior Survival

Among the 90 patients with initial treatment-naive IDH-mutant astrocytomas that were studied, the median overall survival from initial surgery was 8.0 years for those with RAS-MAPK pathway mutation versus 12.1 years for those

without RAS-MAPK pathway mutation. However, likely due to the relative rarity of oncogenic RAS-MAPK pathway mutations in initial resection specimens of IDH-mutant astrocytomas (only 8 patients in this cohort), this survival difference was not statistically significant ( $P = .59$ ; Table 1). Among the 109 recurrent IDH-mutant astrocytomas that were studied, the median survival from surgically treated recurrence was 1.2 years for those with RAS-MAPK pathway mutation versus 3.5 years for those without RAS-MAPK pathway mutation ( $P = .01$ ; Table 1, Figure 5A). Among the 76 recurrent IDH-mutant astrocytomas designated as CNS WHO grade 4 based on the 2021 WHO Classification, the median survival from surgically treated recurrence was 1.0 years for those with RAS-MAPK pathway mutation versus 3.1 years for those without RAS-MAPK pathway mutation ( $P < .01$ ; Supplementary Figure S2A). Among the 70 recurrent IDH-mutant astrocytomas designated as WHO grade IV based on histologic features only using the 2016 WHO Classification criteria, the median survival from surgically treated recurrence was 1.1 years for those with RAS-MAPK pathway mutation versus 3.1 years for those without RAS-MAPK pathway mutation ( $P < .01$ ; Supplementary Figure S2B). Among the 43 recurrent IDH-mutant astrocytomas harboring *CDKN2A* homozygous deletion, the presence of oncogenic RAS-MAPK pathway alteration was associated with inferior survival with median survival from surgically treated recurrence of 0.9 years versus 2.8 years ( $P < .001$ ; Figure 5B). Among the 18 patients with recurrent IDH-mutant astrocytomas harboring oncogenic RAS-MAPK pathway alterations, the presence of *CDKN2A* homozygous deletion was associated with a trend towards inferior survival with median survival from surgically treated recurrence of 0.9 years versus 1.9 years ( $P = .08$ ; Figure 5C). Multivariate analysis demonstrated that oncogenic RAS-MAPK pathway alterations were independently associated with inferior survival for patients with surgically treated recurrent IDH-mutant astrocytoma (hazard ratio = 2.83,  $P < .01$ ; Figure 5D).

## Discussion

Here we confirm recent reports demonstrating that while the vast majority of IDH-mutant astrocytomas are sporadic/spontaneous tumors, a small subset of patients (~3% in this cohort) have tumors arising in the setting of specific tumor predisposition syndromes (Li-Fraumeni syndrome, Ollier syndrome, and Lynch syndrome) due to constitutional pathogenic variants in the *TP53*, *IDH1*, and mismatch repair genes (*MSH2*, *MSH6*, *MLH1*, and *PMS2*).<sup>6,7</sup> These constitutional variants can either be inherited in the germline or arise de novo during embryogenesis associated with constitutional mosaicism. Paired tumor-normal sequencing enabling accurate discrimination of the somatic versus constitutional/germline origin of identified DNA sequence variants is useful for detecting these patients with IDH-mutant astrocytomas arising due to underlying tumor predisposition syndromes. This identification of patients with underlying tumor predisposition syndromes can enable genetic counseling about future cancer risk to affected family members including siblings

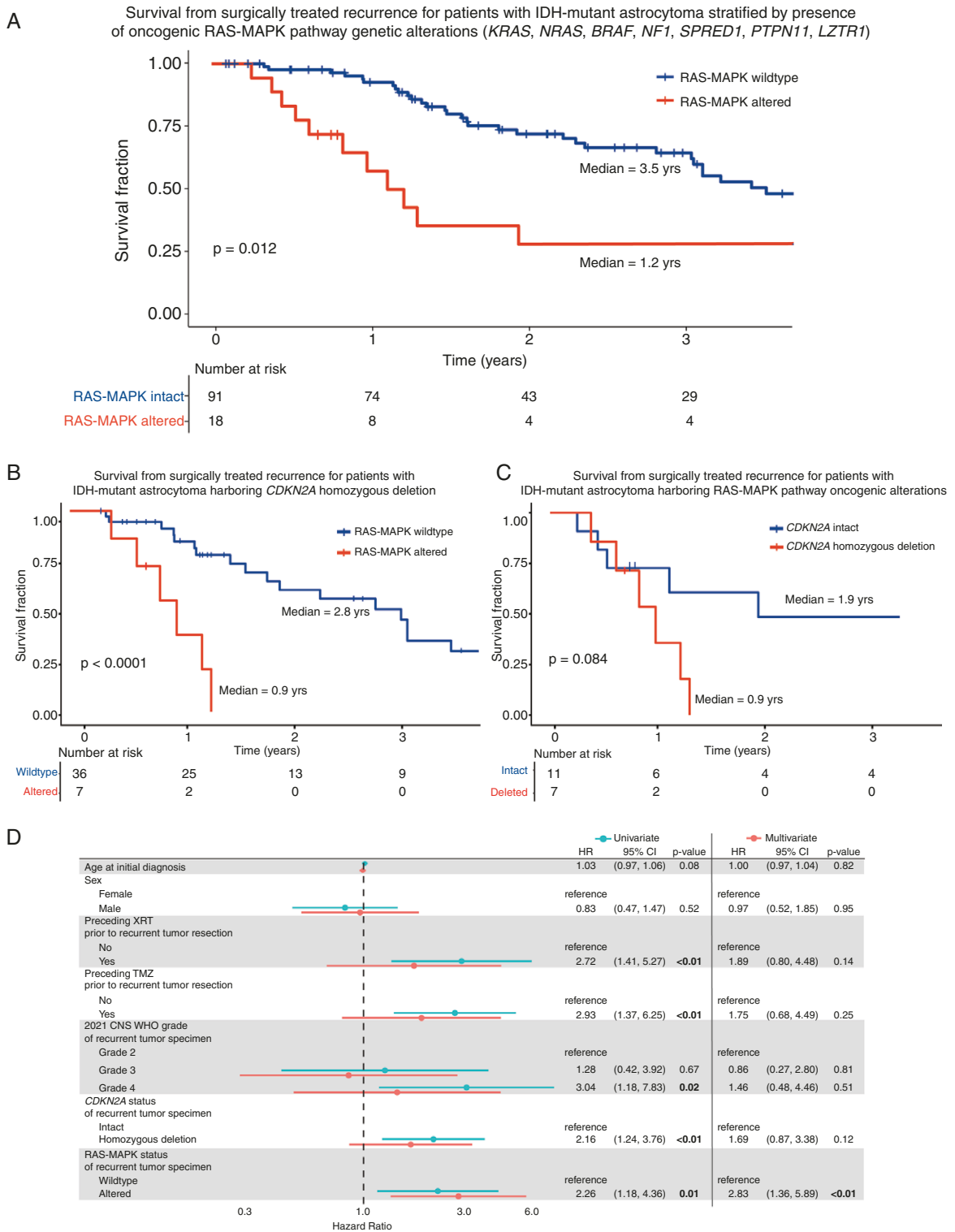


**Figure 5.** Oncogenic RAS-MAPK pathway genetic alterations are associated with inferior survival in patients with recurrent IDH-mutant astrocytoma. (A) Kaplan–Meier plot showing survival from surgically treated recurrence for 109 IDH-mutant astrocytomas stratified by presence or absence of oncogenic RAS-MAPK pathway alterations involving *KRAS*, *NRAS*, *BRAF*, *NF1*, *SPRED1*, *PTPN11*, or *LZTR1*. (B) Kaplan–Meier plot showing survival from surgically treated recurrence for 43 IDH-mutant astrocytomas harboring *CDKN2A* homozygous deletion stratified by presence or absence of oncogenic RAS-MAPK pathway alterations. (C) Kaplan–Meier plot showing survival from surgically treated recurrence for 18 IDH-mutant astrocytomas harboring oncogenic RAS-MAPK pathway alteration stratified by presence or absence of *CDKN2A* homozygous deletion. (D) Univariate and multivariate Cox proportional hazard regression analysis of overall survival from surgically treated recurrence for patients with recurrent IDH-mutant astrocytoma ( $n = 109$ ).

and offspring, as well as enable potentially life-saving cancer surveillance such as colonoscopy, screening MRI, and emerging cell-free DNA screening.<sup>56,57</sup>

Furthermore, IDH-mutant astrocytomas arising in the setting of these different tumor predisposition syndromes may be biologically different than their sporadic counterparts and warrant different prognostic counseling and treatment regimens. For example, IDH-mutant astrocytomas arising in patients with constitutional/germline mismatch repair gene mutation (i.e. Lynch syndrome) have been demonstrated to compose a unique DNA methylation cluster distinct from sporadic IDH-mutant astrocytomas with intact mismatch repair activity and are associated with poor prognosis compared to patients with sporadic IDH-mutant astrocytomas.<sup>7</sup> These unique tumors have been termed “primary mismatch repair deficient IDH-mutant astrocytoma” and should likely be considered a distinct subtype of IDH-mutant astrocytoma moving forward, for which the clinical utility of temozolomide versus other chemotherapeutic agents including immune checkpoint blockade needs to be tested. Both of the 2 patients in this cohort with IDH-mutant astrocytomas arising in the setting of Lynch syndrome due to heterozygous constitutional *MSH2* inactivating mutations had poor outcomes (survival less than 2 years from initial diagnosis), similar to that reported in this prior study.<sup>7</sup> In contrast, both of the patients in this cohort with IDH-mutant astrocytomas arising in the setting of Li-Fraumeni syndrome due to heterozygous constitutional *TP53* mutations had favorable survival and remained alive at last clinical follow-up at ~5 and ~7 years after initial glioma diagnosis. This is similar to a prior study demonstrating favorable outcomes of IDH-mutant astrocytomas arising in the setting of Li-Fraumeni syndrome compared to other patients (usually pediatric) with IDH-wildtype gliomas arising in the setting of Li-Fraumeni syndrome.<sup>6</sup> We also document the genetic composition of an IDH-mutant astrocytoma arising in the setting of Ollier disease due to constitutional mosaicism for *IDH1* p.R132H mutation, revealing additional somatic *TP53*, *ATRX*, *NF1*, *SPRED1*, and *NOTCH1* oncogenic/pathogenic mutations. It remains uncertain why a subset of IDH-mutant astrocytomas arise in the setting of these specific tumor predisposition syndromes, but have not been observed to occur in the setting of other syndromes where primary brain tumors frequently occur such as neurofibromatosis type 1 (NF1) and familial melanoma-astrocytoma syndrome (now termed *CDKN2A*-related tumor predisposition syndrome).

Genetic events underlying malignant progression and high-grade transformation for IDH-mutant astrocytomas have been incompletely defined. Prior longitudinal genomic profiling studies have documented that *IDH1*, *TP53*, and *ATRX* are the earliest mutational events in IDH-mutant astrocytomas that give rise to a low-grade astrocytoma (CNS WHO grade 2).<sup>21,22</sup> The accumulation of additional genetic perturbations affecting cell cycle regulation (e.g. *CDKN2A* homozygous deletion, *CDK4* amplification) and growth factor signaling (e.g. *PDGFRA* amplification, *PTPRZ1::MET* fusion) have been identified as genetic perturbations that are found in IDH-mutant astrocytomas at time of recurrence and high-grade transformation and are associated with inferior survival compared to IDH-mutant

astrocytomas lacking these additional genetic alterations.<sup>23,24,26,27,31,32,34</sup>

Here we identified novel genetic alterations driving activation of the RAS-MAPK mitogenic signaling pathway in a substantial subset of IDH-mutant astrocytomas, which were enriched in those tumors with high-grade histologic features and also in recurrent tumors compared to initial treatment-naïve tumors (17% vs. 9%). Genetic evolution analysis of multiple longitudinal tumor samples from individual patients revealed that these RAS-MAPK pathway mutations occurred during tumor progression subsequent to the earlier initiating *IDH1*, *TP53*, and *ATRX* mutational events (Figure 3). Immunohistochemistry for phospho-ERK1/2 demonstrated evidence supporting RAS-MAPK signaling pathway activation in IDH-mutant astrocytomas with the diverse oncogenic alterations in RAS-MAPK pathway genes (Figure 4). Together, these findings indicate that the RAS-MAPK mutational events are likely to be an underlying contributor of high-grade transformation and treatment resistance for IDH-mutant astrocytomas, probably in cooperation with other such events that have been previously identified such as *CDKN2A* deletion and *PDGFRA* amplification. While each individual RAS-MAPK gene was only altered in a small percentage of tumor specimens, the cumulative frequency of oncogenic RAS-MAPK pathway alterations in this cohort of recurrent IDH-mutant astrocytomas was nearly 20%, potentially explaining why prior longitudinal genomics studies of IDH-mutant gliomas have not focused on these RAS-MAPK events. Notably, RAS-MAPK pathway mutations are known hallmarks of other CNS tumor types (e.g. *BRAF* mutation/fusion in ganglioglioma and pilocytic astrocytoma, *KRAS* mutation in tectal glioma, *NF1* mutation/deletion in gliomas arising in the setting of neurofibromatosis type 1 and a subset of sporadic IDH-wildtype glioblastomas).<sup>46,58-61</sup> However, this is the first study to our knowledge to identify and focus on the significance of RAS-MAPK pathway mutations in IDH-mutant astrocytomas.

Our analysis demonstrated that patients whose recurrent IDH-mutant astrocytomas harbored oncogenic RAS-MAPK pathway alterations had significantly worse survival compared to those with RAS-MAPK wild-type tumors. The combination of oncogenic RAS-MAPK pathway mutation and *CDKN2A* homozygous deletion was associated with markedly poor outcomes beyond *CDKN2A* deletion in isolation, with multivariate analysis demonstrating that RAS-MAPK pathway mutation was an independent prognostic factor after adjusting for other relevant clinical and molecular variables. These findings suggest that oncogenic RAS-MAPK pathway alterations are a significant contributor to the malignant transformation and poor prognosis of patients with recurrent IDH-mutant astrocytomas, underscoring their potential as a valuable prognostic biomarker and potential therapeutic target in this patient population.

In addition to the novel RAS-MAPK pathway genetic alterations, our longitudinal genomic analysis also identified an increased frequency of likely oncogenic alterations targeting the *NOTCH1* and *CIC* tumor suppressor genes in recurrent versus initial treatment-naïve IDH-mutant astrocytomas (Figure 2B). Interestingly, while *NOTCH1* and *CIC* are more well recognized as recurrently mutated

genes in oligodendrogliomas, our finding of *NOTCH1* and *CIC* mutations in a small subset of recurrent IDH-mutant astrocytomas indicates that these 2 genes may also play a role in the progression and treatment response of astrocytomas.

Notably, this study was conducted at a single institution and validation of these findings in additional independent patient cohorts will be essential to confirm the ultimate frequency and prognostic significance of RAS-MAPK alterations in IDH-mutant astrocytomas. Further research using cell or xenograft models of IDH-mutant gliomas expressing RAS-MAPK pathway mutations will help elucidate the specific mechanisms by which these alterations drive tumor aggressiveness and therapeutic vulnerability. At present, no predictive biomarkers have been identified for reliably determining which patients will acquire RAS-MAPK pathway mutation during their disease course, but this may potentially be elucidated through further multi-omic profiling studies examining for DNA methylation or gene expression differences between initial IDH-mutant astrocytoma tumor specimens that do or do not subsequently acquire these alterations at recurrence.

In summary, we have identified a new critical role of RAS-MAPK pathway alterations in the progression of IDH-mutant astrocytomas. Our findings reveal that these RAS-MAPK pathway mutations are typically absent in the initial resection of a low-grade IDH-mutant astrocytoma and are acquired later during gliomagenesis in predominantly high-grade and recurrent tumors. They frequently co-occur with other key oncogenic events known to correlate with inferior survival in IDH-mutant astrocytomas including *CDKN2A* homozygous deletion and *PIK3CA* mutation. Nonetheless, we found in multivariate analysis that these oncogenic RAS-MAPK pathway mutations are independently correlated with inferior survival in patients with recurrent IDH-mutant astrocytoma and should therefore be considered as a potential prognostic determinant for future molecularly integrated grading schemes for IDH-mutant astrocytomas. Future studies are needed to determine how to best treat such IDH-mutant astrocytomas with RAS-MAPK pathway mutations, considering that activation of this mitogenic signaling pathway may be driving resistance to conventional radiation and temozolomide chemotherapy and also be associated with sensitivity to particular targeted therapy agents such as RAS or MEK inhibitors. Furthermore, the molecular determinants of sensitivity and resistance to the newly FDA-approved IDH mutant small molecule inhibitors remain to be determined, and whether these RAS-MAPK pathway mutations determine which patients will respond successfully or who might need combinatorial multi-agent treatment will be important to investigate.

## Supplementary material

Supplementary material is available online at *Neuro-Oncology Advances* (<https://academic.oup.com/noa>).

## Keywords

astrocytoma | glioma | *IDH1* mutation | RAS-MAPK signaling pathway | molecular neuropathology

## LAY SUMMARY

Isocitrate dehydrogenase (IDH)-mutant astrocytomas are brain tumors that usually occur in young adults. While these tumors often grow slowly at first, they can become more aggressive over time. The authors of this study wanted to understand the genetic changes that make these tumors grow faster and resist treatment. To do this they studied tumor genetic changes in the tumors of 172 patients with IDH-mutant astrocytomas. They focused on a set of genes within the RAS-MAPK pathway that control cell growth. Their results showed that 13% of the tumors had changes in these genes. These changes were more common in aggressive tumors and were linked to shorter survival in patients.

## Funding

This study was supported by the UCSF Glioblastoma Precision Medicine Program sponsored by the Sandler Foundation. E.R.A. was supported by the Helen Diller Family Comprehensive Cancer Center Molecular Oncology Program Award. D.A.S. was also supported by the Gilbert Family Foundation, the Morgan Adams Foundation, the Ross Family, the UCSF Department of Pathology Experimental Neuropathology Endowment Fund, and the UCSF Program for Breakthrough Biomedical Research. A.P., J.J.P., and the UCSF Brain Tumor Center Biorepository and Pathology Core were also supported by the UCSF Brain Tumor SPOR (P50 CA097257).

## Acknowledgments

We thank the staff of the UCSF Clinical Cancer Genomics Laboratory, the UCSF Histology Laboratory, and the UCSF Brain Tumor Center Biorepository and Pathology Core for technical assistance. We also thank our patients (the study participants) and the many providers and clinical staff at the UCSF Brain Tumor Center involved in the multidisciplinary care of these neuro-oncology patients.

## Conflict of interest statement

Jennie Taylor receives grant support from Bristol Myers Squibb and Servier Pharmaceuticals and serves on the advisory board for Servier Pharmaceuticals. The remaining authors declare that they have no competing interests related to this study.

## Authorship statement

All authors made substantial contributions to the conception or design of the study; the acquisition, analysis, or interpretation of data; or drafting and revising the manuscript. All authors approved the manuscript. Clinical data extraction and statistical analysis were performed by ERA, GAG, NNA, AD, DQ, and DAS. Genomic analysis was performed by DAS. Pathologic assessment was performed by MP, AP, AWB, JJP, and DAS. Neuro-oncologic patient management was performed by JWT, NAOB, JLC, NAB, JDG, and SMC. Neurosurgical patient management was performed by JSY, EFC, SLHJ, and MSB. Statistical analysis was supervised by AWS and DVG. The study was supervised by JFC, SSF, SMC, and DAS. The manuscript and figures were prepared by ERA and DAS with input from all authors.

## Ethical approval

This study was approved by the Committee on Human Research of the University of California, San Francisco, with a waiver of patient consent.

## Data availability

Patient-level clinical and treatment data are provided in the [supplementary data](#) tables. Annotated DNA sequencing data from the longitudinal IDH-mutant astrocytoma cohort are provided in the [supplementary data](#) tables. Raw sequencing data files are available from the authors upon request.

## Affiliations

UCSF Brain Tumor Center, University of California, San Francisco, California, USA (E.R.A., G.A.G., N.N.A.-A., J.S.Y., A.D., D.Q., J.W.T., N.A.O.B., J.L.C., N.A.B., J.G., M.P., A.P., A.W.B., J.J.P., J.F.C., E.F.C., S.H.-J., M.S.B., S.S.F., S.M.C., D.A.S.); Division of Neuro-Oncology, Department of Neurological Surgery, University of California, San Francisco, California, USA (E.R.A., J.W.T., N.A.O.B., J.L.C., N.A.B., J.G., S.M.C.); Department of Epidemiology and Biostatistics, University of California, San Francisco, California, USA (E.R.A., G.A.G., A.W.S., D.V.G.); Department of Neurological Surgery, University of California, San Francisco, California, USA (N.N.A.-A., J.S.Y., A.D., D.Q., A.P., J.J.P., J.F.C., E.F.C., S.H.-J., M.S.B., S.S.F.); Department of Neurology, University of California, San Francisco, California, USA (J.W.T., N.A.O.B., J.L.C.); Department of Pathology, University of California, San Francisco, California, USA (M.P., A.P., A.W.B., J.J.P., D.A.S.)

## References

- Louis DN, Perry A, Wesseling P, et al. The 2021 WHO classification of tumors of the central nervous system: a summary. *Neuro Oncol.* 2021;23(8):1231–1251.
- Ferris SP, Goode B, Joseph NM, et al. IDH1 mutation can be present in diffuse astrocytomas and giant cell glioblastomas of young children under 10 years of age. *Acta Neuropathol.* 2016;132(1):153–155.
- Yeo KK, Alexandrescu S, Cotter JA, et al. Multi-institutional study of the frequency, genomic landscape, and outcome of IDH-mutant glioma in pediatrics. *Neuro-Oncology.* 2022;25(1):199–210.
- Lim-Fat MJ, Cotter JA, Touat M, et al. A comparative analysis of IDH-mutant glioma in pediatric, young adult, and older adult patients. *Neuro-Oncology.* 2024;26(12):2364–2376.
- Banan R, Stichel D, Bleck A, et al. Infratentorial IDH-mutant astrocytoma is a distinct subtype. *Acta Neuropathol.* 2020;140(4):569–581.
- Sloan EA, Hilz S, Gupta R, et al. Gliomas arising in the setting of Li-Fraumeni syndrome stratify into two molecular subgroups with divergent clinicopathologic features. *Acta Neuropathol.* 2020;139(5):953–957.
- Suwala AK, Stichel D, Schrimpf D, et al. Primary mismatch repair deficient IDH-mutant astrocytoma (PMMRDIA) is a distinct type with a poor prognosis. *Acta Neuropathol.* 2020;141(1):85–100.
- Bonnet C, Thomas L, Psimaras D, et al. Characteristics of gliomas in patients with somatic IDH mosaicism. *Acta Neuropathol Commun.* 2016;4:31.
- Miller JJ, Castro LNG, McBrayer S, et al. Isocitrate dehydrogenase (IDH) mutant gliomas: a Society for Neuro-Oncology (SNO) consensus review on diagnosis, management, and future directions. *Neuro-Oncology.* 2022;25(1):4.
- Mellinghoff IK, Lu M, Wen PY, et al. Vorasidenib and ivosidenib in IDH1-mutant low-grade glioma: a randomized, perioperative phase 1 trial. *Nat Med.* 2023;29(3):615–622.
- Mellinghoff IK, van den Bent MJ, Blumenthal DT, et al. Vorasidenib in IDH1- or IDH2-mutant low-grade glioma. *N Engl J Med.* 2023;389(7):589.
- Turcan S, Rohle D, Goenka A, et al. IDH1 mutation is sufficient to establish the glioma hypermethylator phenotype. *Nature.* 2012;483(7390):479–483.
- Dang L, White DW, Gross S, et al. Cancer-associated IDH1 mutations produce 2-hydroxyglutarate. *Nature.* 2009;462(7274):739–744.
- Watanabe T, Nobusawa S, Kleihues P, Ohgaki H. IDH1 mutations are early events in the development of astrocytomas and oligodendrogliomas. *Am J Pathol.* 2009;174(4):1149–1153.
- Mukherjee J, Johannessen TC, Ohba S, et al. Mutant IDH1 cooperates with ATRX Loss to drive the alternative lengthening of telomere phenotype in glioma. *Cancer Res.* 2018;78(11):2966–2977.
- Liu XY, Gerdes N, Korshunov A, et al. Frequent ATRX mutations and loss of expression in adult diffuse astrocytic tumors carrying IDH1/IDH2 and TP53 mutations. *Acta Neuropathol.* 2012;124(5):615–625.
- The Cancer Genome Atlas Research Network. Comprehensive, integrative genomic analysis of diffuse lower-grade gliomas. *N Engl J Med.* 2015;372(26):2481–2498.
- Ceccarelli M, Barthel FP, Malta TM, et al; TCGA Research Network. Molecular profiling reveals biologically discrete subsets and pathways of progression in diffuse glioma. *Cell.* 2016;164(3):550–563.
- Varn FS, Johnson KC, Martinek J, et al; GLASS Consortium. Glioma progression is shaped by genetic evolution and microenvironment interactions. *Cell.* 2022;185(12):2184–2199.e16.
- Barthel FP, Johnson KC, Varn FS, et al; GLASS Consortium. Longitudinal molecular trajectories of diffuse glioma in adults. *Nature.* 2019;576(7785):112–120.
- Johnson BE, Mazar T, Hong C, et al. Mutational analysis reveals the origin and therapy-driven evolution of recurrent glioma. *Science.* 2013;343(6167):189–193.
- Suzuki H, Aoki K, Chiba K, et al. Mutational landscape and clonal architecture in grade II and III gliomas. *Nat Genet.* 2015;47(5):458–468.
- Shirahata M, Ono T, Stichel D, et al. Novel, improved grading system(s) for IDH-mutant astrocytic gliomas. *Acta Neuropathol.* 2018;136(1):153–166.

24. Appay R, Dehais C, Maura CA, et al; POLA Network. CDKN2A homozygous deletion is a strong adverse prognosis factor in diffuse malignant IDH-mutant gliomas. *Neuro-Oncology*. 2019;21(12):1519–1528.
25. Weller M, Felsberg J, Hentschel B, et al. Improved prognostic stratification of patients with isocitrate dehydrogenase-mutant astrocytoma. *Acta Neuropathol*. 2024;147(1):11.
26. Galbraith K, Garcia M, Wei S, et al. Prognostic value of DNA methylation subclassification, aneuploidy, and CDKN2A/B homozygous deletion in predicting clinical outcome of IDH mutant astrocytomas. *Neuro-Oncology*. 2024;26(6):1042–1051.
27. Yang RR, Shi Z, Zhang Z, et al. IDH mutant lower grade (WHO Grades II/III) astrocytomas can be stratified for risk by CDKN2A, CDK4 and PDGFRA copy number alterations. *Brain Pathol*. 2019;30(3):541–553.
28. Richardson TE, Walker JM. CCND2 amplification is an independent adverse prognostic factor in IDH-mutant lower-grade astrocytoma. *Clin Neuropathol*. 2021;40(4):209–214.
29. Sahm F, Korshunov A, Schrimpf D, et al. Gain of 12p encompassing CCND2 is associated with gemistocytic histology in IDH mutant astrocytomas. *Acta Neuropathol*. 2017;133(2):325–327.
30. Rautajoki KJ, Jaatinen S, Hartewig A, et al. Genomic characterization of IDH-mutant astrocytoma progression to grade 4 in the treatment setting. *Acta Neuropathol Commun*. 2023;11(1):176.
31. Phillips JJ, Aranda D, Ellison DW, et al. PDGFRA amplification is common in pediatric and adult high-grade astrocytomas and identifies a poor prognostic group in IDH1 mutant glioblastoma. *Brain Pathol*. 2013;23(5):565–573.
32. Hu H, Mu Q, Bao Z, et al. Mutational landscape of secondary glioblastoma guides MET-targeted trial in brain tumor. *Cell*. 2018;175(6):1665–1678.e18.
33. Bao ZS, Chen HM, Yang MY, et al. RNA-seq of 272 gliomas revealed a novel, recurrent PTPRZ1-MET fusion transcript in secondary glioblastomas. *Genome Res*. 2014;24(11):1765–1773.
34. Liu L, Zhang KN, Zhao Z, et al. MET fusions and splicing variants is a strong adverse prognostic factor in astrocytoma, isocitrate dehydrogenase mutant. *Brain Pathol*. 2023;34(3):e13198.
35. Lee K, Kim SI, Kim EE, et al. Genomic profiles of IDH-mutant gliomas: MYCN-amplified IDH-mutant astrocytoma had the worst prognosis. *Sci Rep*. 2023;13(1):6761.
36. Mohamed E, Kumar A, Zhang Y, et al. PI3K/AKT/mTOR signaling pathway activity in IDH-mutant diffuse glioma and clinical implications. *Neuro-Oncology*. 2022;24(9):1471–1481.
37. Mirchia K, Sathe AA, Walker JM, et al. Total copy number variation as a prognostic factor in adult astrocytoma subtypes. *Acta Neuropathol Commun*. 2019;7(1):92.
38. Cimino PJ, Zager M, McFerrin L, et al. Multidimensional scaling of diffuse gliomas: application to the 2016 World Health Organization classification system with prognostically relevant molecular subtype discovery. *Acta Neuropathol Commun*. 2017;5(1):39.
39. Choi S, Yu Y, Grimmer MR, et al. Temozolomide-associated hypermutation in gliomas. *Neuro-Oncology*. 2018;20(10):1300–1309.
40. Yu Y, Villanueva-Meyer J, Grimmer MR, et al. Temozolomide-induced hypermutation is associated with distant recurrence and reduced survival after high-grade transformation of low-grade IDH-mutant gliomas. *Neuro-Oncology*. 2021;23(11):1872–1884.
41. Touat M, Li YY, Boynton AN, et al. Mechanisms and therapeutic implications of hypermutation in gliomas. *Nature*. 2020;580(7804):517–523.
42. Kline CN, Joseph NM, Grenert JP, et al. Targeted next-generation sequencing of pediatric neuro-oncology patients improves diagnosis, identifies pathogenic germline mutations, and directs targeted therapy. *Neuro-Oncology*. 2016;19(5):now254.
43. Lucas CHG, Gupta R, Doo P, et al. Comprehensive analysis of diverse low-grade neuroepithelial tumors with FGFR1 alterations reveals a distinct molecular signature of rosette-forming glioneuronal tumor. *Acta Neuropathol Commun*. 2020;8(1):151.
44. Zhang Y, Lucas CHG, Young JS, et al. Prospective genomically guided identification of “early/evolving” and “undersampled” IDH-wildtype glioblastoma leads to improved clinical outcomes. *Neuro-Oncology*. 2022;24(10):1749–1762.
45. Hadad S, Gupta R, Bush NAO, et al. “De novo replication repair deficient glioblastoma, IDH-wildtype” is a distinct glioblastoma subtype in adults that may benefit from immune checkpoint blockade. *Acta Neuropathol*. 2023;147(1):3.
46. Lucas CHG, Sloan EA, Gupta R, et al. Multiplatform molecular analyses refine classification of gliomas arising in patients with neurofibromatosis type 1. *Acta Neuropathol*. 2022;144(4):747–765.
47. Talevich E, Shain AH, Botton T, Bastian BC. CNVkit: genome-wide copy number detection and visualization from targeted DNA sequencing. *PLoS Comput Biol*. 2016;12(4):e1004873.
48. Niu B, Ye K, Zhang Q, et al. MSIsensor: microsatellite instability detection using paired tumor-normal sequence data. *Bioinformatics*. 2013;30(7):1015–1016.
49. Alexandrov LB, Nik-Zainal S, Wedge DC, et al; Australian Pancreatic Cancer Genome Initiative. Signatures of mutational processes in human cancer. *Nature*. 2013;500(7463):415–421.
50. Campbell BB, Light N, Fabrizio D, et al. Comprehensive analysis of hypermutation in human cancer. *Cell*. 2017;171(5):1042–1056.e10.
51. Brems H, Chmara M, Sahbatou M, et al. Germline loss-of-function mutations in SPRED1 cause a neurofibromatosis 1-like phenotype. *Nat Genet*. 2007;39(9):1120–1126.
52. Bigenzahn JW, Collu GM, Kartnig F, et al. LZTR1 is a regulator of RAS ubiquitination and signaling. *Science*. 2018;362(6419):1171–1177.
53. Steklov M, Pandolfi S, Baietti MF, et al. Mutations in LZTR1 drive human disease by dysregulating RAS ubiquitination. *Science*. 2018;362(6419):1177–1182.
54. Liu J, Cao S, Imbach KJ, et al; Philadelphia Coalition for a Cure. Multi-scale signaling and tumor evolution in high-grade gliomas. *Cancer Cell*. 2024;42(7):1217–1238.e19.
55. Zwaig M, Baguette A, Hu B, et al. Detection and genomic analysis of BRAF fusions in Juvenile Pilocytic Astrocytoma through the combination and integration of multi-omic data. *BMC Cancer*. 2022;22(1):1297.
56. Wong D, Luo P, Oldfield LE, et al. Early cancer detection in Li–Fraumeni syndrome with cell-free DNA. *Cancer Discov*. 2023;14(1):104–119.
57. Greer MLC, States LJ, Malkin D, Voss SD, Doria AS. Update on whole-body MRI surveillance for pediatric cancer predisposition syndromes. *Clin Cancer Res*. 2024;30(22):5021–5033.
58. Pekmezci M, Villanueva-Meyer JE, Goode B, et al. The genetic landscape of ganglioglioma. *Acta Neuropathol Commun*. 2018;6(1):47.
59. Collins VP, Jones DTW, Giannini C. Pilocytic astrocytoma: pathology, molecular mechanisms and markers. *Acta Neuropathol*. 2015;129(6):775–788.
60. Chiang J, Li X, Liu APY, et al. Tectal glioma harbors high rates of KRAS G12R and concomitant KRAS and BRAF alterations. *Acta Neuropathol*. 2019;139(3):601–602.
61. Verhaak RG, Hoadley KA, Purdom E, et al; Cancer Genome Atlas Research Network. An integrated genomic analysis identifies clinically relevant subtypes of glioblastoma characterized by abnormalities in PDGFRA, IDH1, EGFR and NF1. *Cancer Cell*. 2010;17(1):98–110.